Reports

Superconductivity at 45 K in Rb/Tl Codoped C_{60} and C_{60}/C_{70} Mixtures

ZAFAR IQBAL,* RAY H. BAUGHMAN,* B. L. RAMAKRISHNA,
SANDEEP KHARE, N. SANJEEVA MURTHY, HANS J. BORNEMANN,
DONALD E. MORRIS

The appearance of superconductivity at relatively high temperatures in alkali metal–doped C_{60} fullerene provides the challenge to both understand the nature and origin of the superconductivity and to determine the upper limit of the superconducting transition temperature (T_c). Towards the latter goal, it is shown that doping with potassium-thallium and rubidium-thallium alloys in the 400 to 430°C temperature range increases the T_c of C_{60}/C_{70} mixtures to 25.6 K and above 45 K, respectively. Similar increases in T_c were also observed upon analogous doping of pure C_{60}. Partial substitution of potassium with thallium in interstitial sites between C_{60} molecules is suggested by larger observed unit cell parameters than for the K_3C_{60} and K_4C_{60} phases. Contrary to previous results for C_{60} doped with different alkali metals, such expansion does not alone account for the changes in critical temperature.

FOLLOWING THE INITIAL OBSERVATION of superconductivity in potassium-doped C_{60} at 19.3 K by Hebard *et al.* (*1*), superconductivity has been reported (*2–4*) at 28 to 30 K in rubidium-doped C_{60} and at 30 K in cesium-doped C_{60}. Tanigaki *et al.* (*5*) have more recently shown that doping of C_{60} with an alloy of cesium and rubidium results in a superconductor having a transition temperature (T_c) as high as 33 K, which is three to five degrees higher than that reported for Rb_3C_{60} (*2, 3*). Also, Kraus *et al.* (*6*) have attempted the synthesis of $KTl_{1.5}$ doped C_{60}. However, perhaps because of the lower temperatures employed during doping (340°C) relative to those used in the present work, these researchers obtained a lower T_c (17.6 K) for C_{60} doped with the potassium-thallium alloy, than for C_{60} similarly doped using potassium alone.

The increases of T_c that we observed were achieved by relatively high temperature thermal annealing of K-Tl or Rb-Tl alloys in close contact with pure C_{60}, or a C_{60}/C_{70} mixture that was predominantly C_{60}. The fullerene mixture used in most of these experiments was made by generating carbon soot by contact-arc vaporization of a graphite rod in 100 torr He (*7*), followed by extraction of the soot with benzene or toluene. According to chromatographic results, this mixture contains about 80% C_{60} and a remainder that is largely C_{70}. Additional experiments were performed with C_{60} which was obtained by separation of this C_{60}/C_{70} mixture by high pressure liquid chromatography. The synthesis conditions and nominal starting compositions for representative samples are summarized in Table 1. Compositions indicated herein in brackets are nominal starting compositions and not necessarily phase compositions, because the overall metal concentration provided corresponds to the relative amounts of fullerene carbon and metal in the initial reaction mixture. When purified C_{60} was used in the preparations, only the metal components in the composition are enclosed in brackets. The observation of an enhanced T_c phase does not depend upon whether pure C_{60} or a C_{60}/C_{70} mixture was used in the sample preparation.

All synthesis reactions were performed under 10^{-6} torr vacuum in 10-cm to 18-cm long quartz or pyrex tubes having a 3-mm inner diameter. Use of Pyrex tubes is preferred, because Pyrex is much less reactive with alkali metals at high temperatures, and such reaction might effect the relationship between nominal dopant composition and the phase composition of the doped C_{60}. The alloys were synthesized prior to the introduction of the fullerene, and we used as guidance the published metal alloy phase diagrams (*8, 9*). Potassium or rubidium were weighed out in a glass capillary (1.1 mm inner diameter) in a dry box having less than a part per million oxygen, and the open alkali metal containing capillary was inserted into a reaction tube that contained a predetermined amount of thallium. After evacuation and sealing the reaction tube, the alloy was formed by annealing at 340°C or above for 2 to 4 hours. After alloy formation, a predetermined amount of C_{60} or C_{60}/C_{70} (typically 20 to 30 mg) was added to the reaction tube contents (as a powder on top of the alloy at the bottom of the reaction tube) and the reaction tube was resealed under 10^{-6} torr vacuum. For the doping process, the reaction tube was inserted into a uniformly preheated, temperature-controlled furnace. After rapid heat-up in 5 minutes to a first anneal temperature T_1, of typically 400°C, the sample was annealed at this temperature for typically 12 to 16 hours. Thereafter, the sample was typically heated during a 1 hour period to a second annealing temperature, T_2, of typically 430°C. Following annealing at this temperature for typically 16 hours, the sample was furnace cooled (3 hours to 30°C). The an-

Table 1. Nominal sample compositions, doping conditions, and critical temperatures (T_c) of K-Tl and Rb-Tl doped C_{60} superconductors.

Nominal sample composition*	Annealing time (hours) at T_1	T_1 (°C)	Annealing time (hours) at T_2	T_2 (°C)	T_c (K)	
					LFS	SQUID†
$[K_{3.0}Tl_{4.5}C_{60}]$	12	400	16	430	25.6	—
$[K_{3.0}Tl_{4.5}]C_{60}$	12	400	16	430	—	23.2
$[K_{4.0}Tl_{6.0}C_{60}]$	12	400	16	430	23.0	—
$[K_{3.0}Tl_{4.5}C_{60}]$	12	320	16	350	18.0	—
$[Rb_{2.7}Tl_{2.2}C_{60}]$	12	400	16	430	41.5	—
$[Rb_{2.7}Tl_{2.2}]C_{60}$	16	400	6	430	40.0	45.0
$[Rb_{1.2}Tl_{1.7}C_{60}]$	12	400	16	430	38.0	—
$[Rb_{1.0}Tl_{2.0}C_{60}]$	12	400	16	430	—	36.5
$[Rb_{1.0}Tl_{2.0}C_{60}]$	16	400	21	430	—	48.0
$[Rb_{2.0}Tl_{2.5}]C_{60}$‡	12, 6.5	375, 385	9.5	420	—	39.0

*C_{60}/C_{70} was used when all the components are enclosed in brackets; pure C_{60} was used when only the metal components are enclosed in brackets. †T_c determined from zero-field cooled measurements. ‡Sample made using a Pyrex reaction tube.

Z. Iqbal, R. H. Baughman, S. Khare, N. S. Murthy, Allied-Signal Inc., Research and Technology, Morristown, NJ 07962.
B. L. Ramakrishna, Department of Chemistry, Arizona State University, Tempe, AZ 85287.
H. J. Bornemann and D. E. Morris, Morris Research Inc., Berkeley, CA 94704.

*To whom correspondence should be addressed.

nealed samples were measured for superconductivity either in the reaction tubes or after transfer to fresh tubes that were then sealed either under vacuum or under 10^{-2} torr of helium.

The critical superconducting temperatures were determined by measuring the hysteretic low-field signal (LFS) of modulated microwave absorption and by superconducting quantum interference device (SQUID) zero-field-cooled (ZFC) dc-magnetic susceptibility measurements, which were supplemented by field-cooled (FC) magnetic susceptibility measurements. The hysteretic LFS technique has been extensively used in the characterization of superconductors and has been analyzed in depth by Blazey *et al.* and others (*10–12*). This method is contactless and provides a rapid and sensitive way to detect the onset of a superconducting transition. However, the LFS cannot provide the superconducting volume fraction, because the LFS intensity scales only with the nature and amount of flux pinning in the superconducting state (*9, 10*). A modified electron spin resonance spectrometer operating at a 9.2-GHz microwave frequency and modulation amplitudes in the 0.1- to 10-Oe range was used for these measurements (*13, 14*).

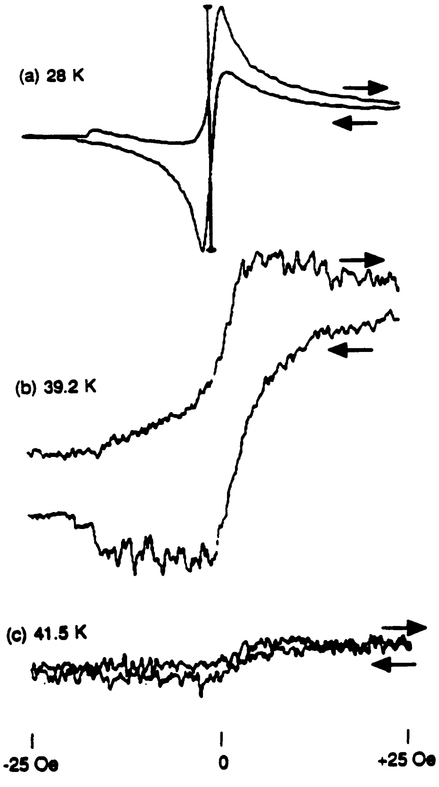

Fig. 1. Hysteretic low field signal spectra for a $[Rb_{2.7}Tl_{2.2}C_{60}]$ sample at (**a**) 28.0, (**b**) 39.2, and (**c**) 41.5 K taken with a 2-Oe modulation amplitude and a 9.3-GHz microwave frequency. Spectra (b) and (c) were scanned at instrumental sensitivity factors of 3.2×10^3 and 2×10^4 times that of spectrum (a). The vertical line indicated on the 28 K spectrum represents the hysteresis intensity at near zero field plotted in Fig. 2.

Figure 1 shows the appearance of typical hysteretic LFS scans (2 Oe modulation) at temperatures below and near T_c for $[Rb_{2.7}Tl_{2.2}C_{60}]$. The signal shape changes with variation in the modulation amplitude from 0.1 to 10 Oe, indicating that the hysteretic LFS is associated with pinned magnetic flux in a granular superconductor (*11*). The hysteretic signal cannot be detected above the background level in our measurements above 41.5 K, which is taken as the onset T_c. The logarithm of the LFS hysteresis intensity near zero-field (shown by the vertical line in Fig. 1a) is plotted in Fig. 2 versus temperature for representative K-Tl and Rb-Tl codoped samples. The data for $[Rb_{3.0}C_{60}]$ prepared under our high temperature synthesis conditions, as well as that for $[K_{3.0}C_{60}]$, are also shown in the figure.

The following discussion together with the results of Table 1 summarizes T_c determinations for different samples made by taking the transition to be the onset of hysteretic LFS. The T_c obtained for $[K_{3.0}C_{60}]$ (T_1 = 200°C, T_2 = 250°C) was 20.0 K, as compared with the literature value of 19.5 K and the T_c obtained for $[Rb_{3.0}C_{60}]$ was 34 K, as compared with the literature value (*3*) of 30 K. This significantly higher T_c obtained with hysteretic LFS for $[Rb_{3.0}C_{60}]$, as compared with the literature result obtained on purified C_{60} with magnetic susceptibility data (*3*), might reflect the greater sensitivity of the hysteretic LFS to flux pinning in minor superconducting fractions of the sample. Flux pinning is expected to be stronger in samples synthesized with C_{60}/C_{70} mixtures compared with samples containing purified C_{60}. Most importantly, a T_c of 25.6 K was obtained for $[K_{3.0}Tl_{4.5}C_{60}]$ and a T_c of 41.5 K was obtained for both $[Rb_{2.7}Tl_{2.2}C_{60}]$ and $[Rb_{2.0}Tl_{1.2}C_{60}]$. Also, using the chromatographically separated C_{60}, we obtained a T_c of 40 K for $[Rb_{2.7}Tl_{2.2}]C_{60}$. A sample with lower relative amounts of Rb to Tl, $[Rb_{1.2}Tl_{1.7}C_{60}]$, provided a lower T_c of 38.0 K. However, a thallium-rich composition annealed for a longer time shows the highest T_c determined from ZFC magnetic susceptibility data (Table 1 and following discussion). These results therefore indicate that if thallium is used as a codopant with potassium and with rubidium the superconductivity onset T_c measured by LFS is increased by 5.6 K and 7.5 K, respectively. The enhanced T_c is also evident in the hysteresis in LFS intensity at 32 K for the $[Rb_{2.7}Tl_{2.2}C_{60}]$ sample, which is two orders of magnitude higher than that for the $[Rb_{3.0}C_{60}]$ sample at this temperature (Fig. 2). The above enhancements in T_c were only observed for doping temperatures (400°C and 430°C) which are much higher than those used by Kraus *et al.* (*6*) in their efforts to dope C_{60} using a K-Tl alloy. For example, when lower reaction temperatures (T_1 = 320 K and T_2 = 350 K) are employed for a $[K_{3.0}Tl_{4.5}C_{60}]$ sample, the T_c is 18.0 K (see Table 1), in agreement with the results of Kraus *et al.* (*6*). The reliability of our above measurements was checked by measuring T_c by hysteretic LFS for a single crystal of the cubic bismuthate superconductor ($Ba_{1-x}K_xBiO_3$) which shows 100% diamagnetic shielding by magnetometry and a sharp onset at a T_c of 32 K. Experiments during both heating and cooling provided a T_c which was within 1 K of the above value.

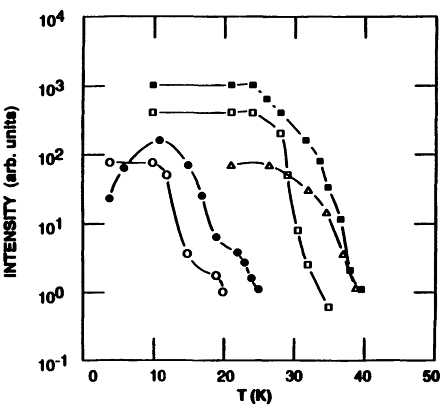

Fig. 2. Plot of the logarithm of the hysteresis intensity (defined in the Fig. 1 caption) versus temperature (K) for (■) $[Rb_{2.7}Tl_{2.2}C_{60}]$, (△) $[Rb_{2.0}Tl_{1.3}C_{60}]$, (□) $[Rb_{3.0}C_{60}]$, (●) $[K_{3.0}Tl_{4.5}C_{60}]$, and (○) $[K_{3.0}C_{60}]$. Note that the highest temperature data points represent the onset of measurable hysteresis in our LFS measurements.

DC magnetic susceptibility data (for applied fields between 10 and 90 Oe) on K-Tl and Rb-Tl codoped C_{60} and C_{60}/C_{70} were obtained with a well-calibrated Quantum Design SQUID magnetometer. Due to flux pinning forces, the FC diamagnetic fraction is approximately a factor of seven lower than the ZFC diamagnetic fraction in these samples. A T_c of 43 K and 45 K is indicated by FC and ZFC magnetic susceptibility data, respectively, for $[Rb_{2.7}Tl_{2.2}]C_{60}$. This latter data (Fig. 3) shows a clear onset to superconductivity at 45 K and a shielding diamagnetic fraction of approximately 2.5% at 10 K. A T_c of 39 K with a shielding diamagnetic fraction of about 2% was found by FC and ZFC measurements on a $[Rb_{2.0}Tl_{2.5}]C_{60}$ sample. In the latter sample, the dopant alloy was formed at the congruently melting Rb_4Tl_5 composition (*9*) and the observed FC data shows a sharp transition with onset at 39 K and saturation of the diamagnetic signal near 30 K. For a $[Rb_{1.0}Tl_{2.0}C_{60}]$ sample which was annealed for relatively long times, as indicated in Table 1, a T_c onset as high as 48 K has been observed in ZFC magnetic susceptibility measurements at a field of 90 Oe. Typical diamagnetic fractions obtained for K-Tl doped samples are about 1% at 10 K.

The superconductor fractions presently achieved are about the same as initially reported for K-doped C_{60} and for Rb-doped C_{60} (*1, 2*), although more recent work has dramatically increased the superconductor fraction for C_{60} doped only with alkali metals (*3, 5*). Similar optimization of diamagnetic fraction for the enhanced T_c superconductor in the ternary Rb-Tl-C_{60} or K-Tl-C_{60} systems is much more difficult, not only because of the additional compositional parameter, but also because of the major differences in volatility and ionization potential of the alkali metals and thallium. Also, in order to avoid overdoping which is expected to destroy superconductivity (*17*), the amount of alloy used for doping was sufficiently small that major compositional changes in the dopant alloy likely occur during the doping process. As a consequence of these aspects, the variety of doped phases which can coexist, and the likely combination of liquid phase and vapor doping processes in the present experiments, the synthesis of the high-temperature superconductor phase is sensitive to doping temperatures, total metal concentration, and the ratio of alkali metal to thallium. For example, transition temperature increases (T_c between 36.5 and 48 K) resulting from thallium codoping were observed for seven samples having a nominal Tl/C_{60} ratio between 1.3 and 2.5, a nominal Tl/Rb ratio between 0.6 and 2.0, and a highest annealing temperature during doping of between 420° and 430°C (Table 1). However, a lower T_c of 25 to 30 K (and sometimes a slope change for susceptibility at 15 to 20 K, suggestive of a second superconducting component for doped C_{60}/C_{70} mixtures) was observed for samples with only slightly different nominal compositions or annealing conditions. Even using synthesis conditions in the above ranges, enhanced T_c's were not observed for all preparations. We suspect that liquid alloy contact doping, as opposed to vapor phase doping, is required when using the present isothermal doping method, and that contact of liquid alloy and fullerene did not occur for such preparations which provided the lower T_c's.

X-ray diffraction measurements (with CuKα radiation and samples sealed under argon in Lindemann tubes) on the K-Tl and Rb-Tl alloy-doped C_{60} and C_{60}/C_{70} are consistent with the existence of a mixture of phases which includes various combinations of face-centered-cubic (fcc) undoped C_{60}, a fcc doped phase, a body-centered-tetragonal (bct) doped phase, and a body-centered-cubic (bcc) doped phase. The precise stoichiometries for these doped phases obtained with the alkali metal-thallium codopants is presently unknown, but by analogy with previous work (*15–18*) on C_{60} doped with only the alkali metals, the expected molar ratios of total metal to C_{60} for these phases are expected to be close to 3, 4, and 6, respectively. The unit cell parameters measured for the undoped C_{60} and the C_{60}/C_{70} mixture are essentially the same: a fcc lattice with a = 14.174(12) Å and a = 14.24(5) Å, respectively, compared with the reported a = 14.172 Å for fcc C_{60} (*17*). The unit cell parameter for the fcc phase observed as the predominant phase component in $[K_{3.0}Tl_{4.5}C_{60}]$ is 14.7(1) Å, which is larger than reported (*15, 18*) for either K_3C_{60} [14.253(3) Å] or Rb_3C_{60} [14.436(2) Å]. Increased unit cell parameters were also observed for a minor bct phase component in $[K_{3.0}Tl_{4.5}]C_{60}$, for which a = 12.1 Å and c = 11.3(1) Å, as compared with the previously reported (*17*) a = 11.886(7) Å and c = 10.774(6) Å for K_4C_{60} and a = 11.962 Å and c = 11.022 Å for Rb_4C_{60}. In contrast with these results, the bcc phase component in this sample provides a = 11.4 Å, which is essentially unchanged from the previously reported a = 11.39 Å for K_6C_{60} (*16*). Also, fcc and bct phases observed for $[Rb_{2.7}Tl_{2.2}]C_{60}$ have essentially the same unit cell parameters (a = 14.46 Å and a = 12.0 Å and c = 11.0 Å, respectively) as reported (*17, 18*) for Rb_3C_{60} and Rb_4C_{60}. Because of the superposition of diffraction lines attributable to different phases, as well as the low concentrations of some of the phases, limited comments can be made concerning changes in relative line intensities resulting from codoping with thallium. However, significant changes in relative diffraction intensities were obtained for the expanded fcc phase obtained by K-Tl codoping, as compared with those reported (*15, 18*) for K_3C_{60}. Specifically, the intensities of the (111), (222), and (333) peaks increase relative to that of the (311) peak, which is the strongest diffraction line in K_3C_{60}.

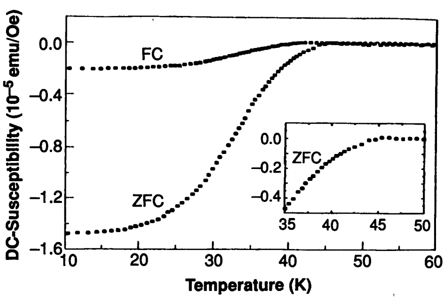

Fig. 3. Zero-field cooled (ZFC) and field-cooled (FC) dc magnetic susceptibility as a function of temperature for a 20-mg $[Rb_{2.7}Tl_{2.2}]$ C_{60} sample at fields of 60 Oe and 50 Oe, respectively. The inset shows a detailed plot of the ZFC data near T_c, indicating a T_c of 45 K.

The above reported lattice expansions and intensity changes suggest that the thallium partially replaces potassium ions that occupy octahedral and tetrahedral holes between the C_{60} molecules in the fcc and bct structures. In addition, atomic absorption and chemical analyses of the C_{60} powder separated from unreacted alloy (attached to the reaction tube) from a $[Rb_{2.7}Tl_{2.2}C_{60}]$ preparation shows the presence of thallium and an average composition in the sample corresponding to $Rb_{1.32}Tl_{0.21}C_{60}$. The radii of the tetrahedral holes (two per C_{60}) and octahedral holes (one per C_{60}) in the fcc phase, calculated using the carbon-potassium distances in the K_3C_{60} structure (*15*) and a van der Waals radius of 1.7 Å for carbon, are about 1.57 and 1.99 Å, respectively. Since the ionic radius (*19*) of K^+ (1.33 Å) is smaller than for Tl^+ (1.47 Å), Tl^+ might preferentially occupy the larger octahedral holes. In contrast, Rb^+ and Tl^+ have about the same ionic radius, 1.47 Å (*19*), which might explain the absence of a lattice expansion if thallium is used as a codopant with rubidium. However, thallium is not expected to be completely ionized in $M_{3-y}Tl_yC_{60}$ or $M_{4-y}Tl_yC_{60}$ compositions and the metallic radius of thallium [1.70 Å in thallium and 1.61 Å in Na_2Tl (*20*)] is substantially larger than for Tl^+. A low degree of ionization for the thallium is suggested for the codoped compositions, based on both electrochemical data (*19, 21*) and our inability to observe doping of C_{60} with thallium in the absence of an alkali metal. This electrochemical data indicates that thallium is not able to reduce C_{60} by a three electron process to generate Tl^+ ions and $C_{60}{}^{-3}$. However, cyclopentadienylthallium (I), TlC_5H_5, is an exceptionally stable crystalline complex in which there is considerable charge transfer from the thallium, which sits in the center of a C_5H_5 ring (*20*). Structural similarities might well exist for the thallium-alkali metal codoped C_{60}, because all carbons in C_{60} are in C_5 rings.

The structure of the minority phase component having significantly enhanced T_c is not presently established, so comments concerning the origin of the T_c increases are necessarily speculative. Because the only previously known superconducting phases of C_{60} have the fcc M_3C_{60} type of structure, it is tempting to attribute the enhanced critical temperatures to such phases in which the thallium partially replaces the alkali metal. However, if this assignment is correct, the low observed fraction of superconductor indicates that superconductivity must occur only in an optimally codoped minority component in samples such as [$K_{3.0}Tl_{4.5}C_{60}$], where the majority phase has an expanded doped fcc structure. Fleming *et al.* (*18*) have shown that there is a linear correlation between the T_c of the alkali metal doped C_{60} and the unit cell parameter of the fcc phase, which is explained by band narrowing, resulting in an increased electronic density-of-states at the Fermi level, caused by decreased interactions between C_{60} molecules. Perhaps in part because of incomplete charge transfer from thallium, the transition temperatures observed here are either too low (K-Tl codopants) or too high (Rb-Tl codopants) to be consistent with the abovementioned correlation, assuming that the fcc unit cell parameter measured by x-ray diffraction corresponds to the superconducting fraction with enhanced critical temperatures. The bcc phase is unlikely to be the higher T_c superconducting phase in the thallium codoped samples, because of the absence of any positive correlation between the amount of this phase and the observed superconducting fraction, which is consistent with previous work on alkali metal doped C_{60} (*15, 17, 18*). The remaining observed crystalline phase in the K-Tl and Rb-Tl codoped samples is the bct phase, which is reported not to superconduct when doped only with alkali metals (*17*). However, since this phase is typically observable in small amounts in our superconducting K-Tl and Rb-Tl codoped samples and since our superconducting fractions are low, we cannot exclude the possibility that the enhanced critical temperatures result from a thallium and alkali metal codoped bct C_{60} phase. The answer to these questions regarding the structural nature of the superconducting phase will require the synthesis of thallium codoped superconductor samples with higher fractions of the enhanced critical temperature superconducting phase.

REFERENCES AND NOTES

1. A. F. Hebard *et al.*, *Nature* **350**, 600 (1991).
2. M. J. Rosseinsky *et al.*, *Phys. Rev. Lett.* 66, 2830 (1991).
3. K. Holczer *et al.*, *Science* **252**, 1154 (1991).
4. S. P. Kelty, C. C. Chen, C. M. Lieber, *Nature* **352**, 223 (1991).
5. K. Tanigaki *et al.*, *ibid.*, p. 222.
6. M. Kraus *et al.*, *Z. Phys. B*, in press.
7. W. Krätschmer, L. D. Lamb, K. Fostiropoulos, D. R. Huffman, *Nature* 347, 254 (1990).
8. M. Hansen, *Constitution of Binary Alloys* (McGraw-Hill, New York, 1958) p. 883.
9. R. Thümmel and W. Klemm, *Z. Anorg. Chem.* **376**, 44 (1970).
10. K. W. Blazey, A. M. Portis, J. G. Bednorz, *Solid State Commun.* **65**, 1153 (1988).
11. K. W. Blazey, in *Earlier and Recent Aspects of Superconductivity*, J. G. Bednorz and K. A. Müller, Eds. (Springer-Verlag, New York, 1990), p. 262.
12. F. J. Owens and Z. Iqbal, in *Studies of High Temperature Superconductors*, A. Narlikar, Ed. (Nova Publishers, New York, in press), vol. 9.
13. I. I. Khairullin, A. A. Zakhidov, P. K. Khabibullaev, Z. Iqbal, R. H. Baughman, *Synth. Metals* **33**, 243 (1989).
14. B. L. Ramakrishna, E.-W. Ong, Z. Iqbal, *J. Appl. Phys.* **64**, 5803 (1988).
15. P. W. Stephens *et al.*, *Nature* **351**, 632 (1991).
16. O. Zhou *et al.*, *ibid.*, p. 462.
17. R. M. Fleming *et al.*, *Nature* **352**, 701 (1991).
18. R. M. Fleming *et al.*, *ibid.*, p. 789.
19. *CRC Handbook of Chemistry and Physics*, D. R. Lide Ed. (CRC Press, Boca Raton, FL, ed. 71, 1990), pp. 8-19 and 12-1.
20. A. G. Lee, *The Chemistry of Thallium* (Elsevier, Amsterdam, 1971), pp. 245–246.
21. P. M. Allemand *et al.*, *J. Am. Chem. Soc.* **113**, 1050 (1991).

2 August 1991; accepted 1 October 1991

Liquids at Large Negative Pressures: Water at the Homogeneous Nucleation Limit

Q. ZHENG, D. J. DURBEN, G. H. WOLF, C. A. ANGELL

An isochoric cooling method for obtaining unprecedented tensions on liquids was used to determine the homogeneous nucleation limit for stretching of water at a variety of water densities. At densities in the range 0.55 to 0.68 gram per milliliter (g/ml), the data agree with the homogeneous nucleation temperatures measured by Skripov for superheated water at positive pressures. At densities between 0.68 and 0.93 g/ml, cavitation occurred only at negative pressures (that is, under tension). The cavitation tensions measured were in excellent agreement with those predicted by Fisher's 1948 vapor nucleation theory. A maximum tension of 140 megapascals (=1400 bars) was reached at 42°C, which lies on an extrapolation of the line of isobaric density maxima. At higher densities, cavitation of droplets that survived heterogeneous nucleation failed to occur at all unless provoked, at much lower temperatures, by freezing. This observation confirms the existence of a density maximum at 42°C and −140 megapascals and hence greatly strengthens the basis for Speedy's conjecture of a reentrant spinodal for water.

LIQUIDS UNDER TENSION (THAT IS, at negative pressure) are of interest because their behavior should be dominated by the intermolecular attractive forces rather than by the short-range repulsive (steric) forces, which, according to current theory (*1, 2*), control the structure and dynamics of liquids at normal and high pressures. However, because of the prevalence and efficiency of heterogeneous nuclei for vapor-phase nucleation, the negative-pressure region (metastability with respect to the vapor-liquid coexistence line on the one-component phase diagram) is much less easily investigated than the supercooled liquid region (metastability with respect to the liquid-crystal coexistence line). The particular case of water has, of course, been given the most attention. Despite experimental investigation since the 1840s (*3–8*) and the development of ingenious and sophisticated techniques (*4–8*), there have been no reports of controlled stretching of laboratory samples of water to negative pressures at all comparable to the theoretical limit, which is calculated as −140 MPa at 25°C from homogeneous nucleation theory (*9, 10*) or about −200 MPa at 35°C from spinodal breakdown theory (*11, 12*).

In 1950 Briggs succeeded in reaching −27.7 MPa with a rotating capillary technique (*4*), and Greenspan and Tschiegg (*5*) later reached −25 MPa with an acoustic technique. Henderson and Speedy (*8*) recently measured densities at −19 MPa with a spiral capillary version of Berthelot's original isochoric cooling technique (*3*). These pressure ranges were disappointing, but Roedder (*13*) found evidence for higher tensions in microscopic aqueous inclusions in certain minerals. He reported cases in which ice melted above 0°C, in one case reaching +6.5°C, which, from extrapolations of the melting line, implies a tension of at least 95 MPa in the inclusion. Combining this observation with Apfel and Smith's (*7*) demonstration that negative pressures in good agreement with the theoretical limit for homogeneous nucleation of bubbles of −1.7 MPa at 130°C could be generated in tiny droplets of ether sonically suspended in glycerine, we conjectured that large tensions close to the theoretical limit for bubble nucleation in water of −140 MPa could be obtainable if appropriate microsample techniques were used. Indeed, we recently demonstrated (*14*) that aqueous inclusions (actually saline solutions) found in microdispersed form in quartz crystals could sustain tensions up to 140 MPa. We have now used an inclusion synthesis technique

---

Department of Chemistry, Arizona State University, Tempe, AZ 85287.